Science of Sintering, **51** (2019) 175-187

doi:https://doi.org/10.2298/SOS1902175T

UDK: 546.57; 549.613.4; 53.086

Effect of Silver Nanoparticless in the Structure and Mechanical Properties of Mullite/Ag Cermets

M. Gabriela Téllez-Arias[1,2], José G. Miranda-Hernández[1], Oscar Olea-Mejía[3], J. Lemus-Ruiz[4], Eduardo Terrés[5*)]

[1]Universidad Autónoma del Estado de México (CU-UAEM-VM), Estado de México, México.

[2]Universidad Michoacana de San Nicolás de Hidalgo, (FIQ), Edif. M-CU, Morelia, Michoacán, México.

[3]Universidad Autónoma del Estado de México, Facultad de Química (CCIQS-UAEM-UNAM), Estado de México, México.

[4]Universidad Michoacana de San Nicolás de Hidalgo, (IIMM), Edif. U-CU, Morelia, Michoacán, México.

[5]Instituto Mexicano del Petróleo, México City, México.

Abstract:

The objective of this work was to study the influence of the addition of silver nanoparticles in the microstructure of mullite at two different temperatures of sintering (1500 and 1600 °C), in order to decrease the porosity and increase the density as well better the hardness and fracture toughness. The microstructural characteristics were studied by scanning electron microscopy, confocal scanning microscopy and X-ray diffraction. Mullite/Ag cermets with homogenous microstructure were and a fracture toughness of 2.42 MPa·m$^{1/2}$.

Keywords*: Mullite; Confocal scanning microscopy; Scanning electron microscopy; Homogenous microstructure; Sintering.*

1. Introduction

Mullite ($3Al_2O_3{\cdot}2SiO_2$) is a stable compound in the alumina-silica system and one of the materials in oxide ceramics most widely studied [1-3]. Mullite is an attractive potential engineering ceramic due to high strength and high creep resistance [4-9] as well as other applications at high temperature due to its high-thermal and chemical stability and the excellent thermo-shock behavior [10-14] owing its unique combination of properties like high melting point (1830 °C), low thermal expansion coefficient (4.5 X 10^{-6} K^{-1}), and low dielectric constant (ε = 56.5 at 1 MHz) [1, 12]. However, mullite by itself suffers from low fracture toughness (~ 2MPa $m^{1/2}$) at room temperature and difficulties in sintering to full density material [3, 15-16].

Composite materials formed by metallic particles dispersed within insulating matrix (i.e. ceramic) are known as *cermets* [17]. These composites have recently attracted considerable attention due to a singular combination of dissimilar properties (including mechanical, optical, electrical and magnetic properties) of their components, which make them excellent candidates to fabricate multifunctional devices with new and unique features.

*) **Corresponding author:** eterres@imp.mx

The purpose of the metal reinforcement in the ceramic matrix is to modify the mechanical properties of hardness, fracture toughness and elastic module, considering the nature of the ceramic materials are very hard with low fracture toughness and high elastic module that makes them sensitive to mechanical failure by cracking when these are subjected to mechanical stress by tension, compression or vibration [1, 18-19]. In the case of mullite in order to improve its fracture toughness and as well as another mechanical property has been introduced in their microstructure different metallic particles like W, Mo, Ni, Al, Cr, Ti, Fe, FeO, CoO, Nb, etc [20-25].

Silver matrix composites (SMCs) are a group of Metal Matrix Composites (MMCs) which are widely used in electrical make-break contacts like air conditioner controls, aircraft switches, governor relays and wiping shoes in power transformers [26]. Besides, silver and its compounds are popular antimicrobial agents like nanoparticles are now used in a wide spectrum of consumer products right from clothing, respirators, antibacterial sprays, detergent, socks, shoes, etc. [27], its addition is an option to improve the mechanical and electrical properties of the mullite and to be able to expand its potential applications [28]. This work focused to study different aspects of the addition of silver nanoparticles in the microstructure and mechanical properties of mullite during sintering at 1500 and 1600 °C.

2. Materials and Experimental Procedures

Commercial powders of mullite (98 % pure, <150 μm, Kyanite Mining Corp, USA) and silver nano-powders (99.99 % pure, < 100 nm, Aldrich Products) were used to obtain mullite/Ag cermets materials, the silver concentrations vary from 0, 1, 3, 5, 10, 20 and 30 % wt. In order to develop a homogenous mixture, combination of silver and mullite powders were mixed in a high energy planetary mill for two hours at 200 rpm. High energy promotes a good integration and distribution of the silver inside mullite in the cylindrical compacts (pads) which were obtained via cold compaction with a uniaxial load of 200 MPa priory to sintering process. Mullite/Ag cermets materials were sintered at 1500 and 1600 °C for 60 minutes in a high temperature furnace under controlled nitrogen gas atmosphere to prevent metallic particles oxidation.

Diameter, thickness and volume of the pads were measured to determine the density using the Archimedes method according to ASTM C 20-00 as well as the porosity. The pads corresponding at two sets of mullite/Ag cermets sintered at 1500 and 1600 °C were characterized by X-ray diffraction (XRD) using an X-ray diffractometer PANalytical brand model EMPYREAN in the 2θ range of 10-90 with Cu K_α radiation (λ=0.154056 nm) at 20 KV to detect possible phase transformation. The microstructural analysis of the mullite/Ag cermets was realized by scanning electron microscopy (XL30 ESEM, Philips) coupled with EDS detector. Confocal Microscopy (LMS 710, Zeiss, with lasers of 405, 458, 514, 561, 594 and 633 nm) was realized to know the silver distribution in the matrix of mullite.

The fracture toughness was determined using JIS R 1607 [29], the respected single-edged precrack beam method for determining K_{Ic}, but it also includes a Vickers indentation fracture (IF) method as an alternative to compute a "K_c" parameter. The mechanical evaluation of the samples consisted of microhardness tests in a team (Emco-Test DuraScan 200) with manual turner of the measuring tower with 2 adapter lenses of 10X and 40X, an indenter as a penetrator with a test range of 0.01 to 10 Kgf (0.098-98 N). The determination of the hardness consists in applying a load (P_H) by means of a diamond point indenter of pyramidal shape, when the mark is registered the diagonals of the geometric figure are measured (Fig. 1) and directly the equipment measures the relation of the angles and the diagonals of the fingerprint to determine the hardness measurement, in the Fig. 1 the fingerprint of the indenter is observed and the lines are referenced in the vertices of the break to determine the hardness. The equation to measure the hardness is the following:

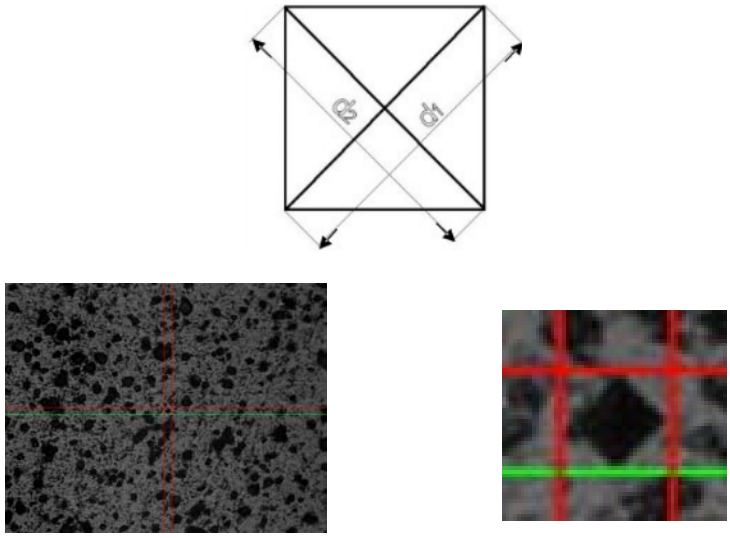

Fig. 1. Diagonals and indentation mark on the material used to determine the hardness.

$$HV = 1.8544\frac{P_H}{d^2} \qquad (1)$$

where:

P_H = Load applied in Kgf
d = The average measure of the diagonal d1 and d2 in mm $d = \frac{d_1+d_2}{2}$

Initially the pads were polished to mirror and 10 indentations were made by cermet, this with the purpose of obtaining an average, using a load of P_H = 0.2 Kgf (1.96N) besides knowing the change in the hardness of the mullite tablets without reinforcement and of mullite with reinforcement with different content of silver nanoparticles.

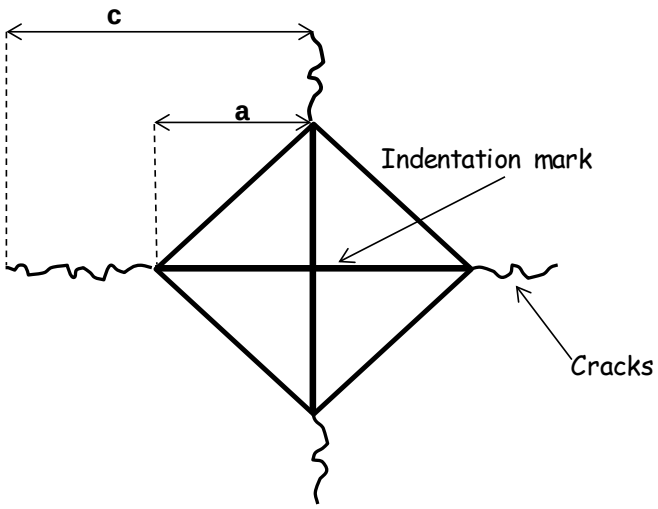

Fig. 2. Vickers Indentation footprint.

Fracture toughness was measured by IF method, obtaining consists in relating the lengths of the cracks generated when applying a load (P_{FT}), which are generated in the vertices of the indentation footprint, as shown in Fig. 2. The test to the fracture toughness

(K_C) was realized in the same way and determined by the equipment of hardness, but now indirectly, that is, a load greater than the hardness on the surface of the material is applied, said load was P_{FT} = 0.5 Kgf (4.90 N), 5 indentations were made by cermet in the different concentrations of Ag at both sintering temperatures. Once the size of the crack "c" and "a" were measured, K_c is determined and made by the relationship of equation 2, the formula known as the Miyoshi equation [30]:

$$K_c = 0.018 \left(\frac{E}{HV}\right)^{0.5} \left(\frac{P_{FT}}{c^{1.5}}\right) \qquad (2)$$

where:

E = Elastic modulus in GPa
HV = Hardness in GPa
P_{FT} = Indentation load in Kgf
c = Crack length in m

Young's modulus or modulus of elasticity (E) measures the material's resistance to elastic deformation. The calculation of this property was made indirectly measuring the speed of sound and the density of the cermets; since the speed of propagation of sound in solids is given by equation 3. To measure the speed of sound we used an equipment brand Ultrasonic Thicknees Gauge (Phase II) model UTG-2008.

$$speed\ of\ sound = \sqrt{\frac{E}{\rho}} \qquad (3)$$

where:

E = Module of young in GPa
ρ = Density in Kg/m^3

We took 7 values of the speed of sound for each cermet in order to determine an average that could be significant. With the help of equation 3, the average value of the measured density ($\rho_{measured}$) and the speed of sound are replaced so that the value of Young's modulus can be calculated.

3. Results and Discussion

Two sets of mullite/Ag cermets were prepared with different proportions of silver (X = 0, 1, 3, 5, 10, 20 and 30 wt.%) at 1500 and 1600 °C, the Archimedes technique was used to measure the density of cermets ($\rho_{measured}$), and the relative density ($\rho_{relative}$) was calculated by the following relation:

$$\rho_{relative} = \frac{\rho_{measured}}{\rho_{theory}} \qquad (4)$$

where: ρ_{theory} is the theoretical density which can be determined from the weight percentage of the phase silver and mullite according to the following equation [15]:

$$\rho_{Theory} = \frac{100}{\frac{X_{silver}}{\rho_{silver}} + \frac{X_{mullite}}{\rho_{mullite}}} \qquad (5)$$

where ρ_{silver} and $\rho_{mullite}$ are the densities of silver and mullite (g/cm^3) with their respective weight percentage, X_{silver} and $X_{mullite}$.

Tab. I shows the results of density and densification of cermets sintered at 1500 and 1600 °C and different silver content. It can be observed that at 1500 °C the $\rho_{measured}$ increases in relation to the increase in Ag content, going from 2.83 g/cm^3 for mullite alone to a value of 3.23 g/cm^3 for cermet with 30 % silver, while at 1600 °C $\rho_{measured}$ values range from 2.86 g/cm^3 for mullite alone to 3.44 g/cm^3 for mullite with 30 % Ag. At 1600 °C, the $\rho_{measured}$ is lightly higher compared to cermets sintered at 1500 °C.

Tab. I Density parameters of mullite/Ag cermets.

Sintered Temperature (°C)	Pads	(A) $\rho_{measured}$ (g/cm^3)	(B) ρ_{theory} (g/cm^3)	(C) $\rho_{relative}$	(D) Densification (%)	(E) Densification by EDS (%)
1500	Mullite	2.83	3.17	0.89	89	89
	Mullite - 1% Ag	2.85	3.19	0.89	89	89
	Mullite - 3% Ag	2.88	3.23	0.89	89	88
	Mullite - 5% Ag	2.91	3.28	0.88	89	88
	Mullite - 10% Ag	2.95	3.40	0.86	86	86
	Mullite - 20% Ag	3.16	3.68	0.85	85	86
	Mullite - 30% Ag	3.23	4.00	0.80	80	86
1600	Mullite	2.86	3.17	0.90	90	90
	Mullite - 1% Ag	2.88	3.19	0.90	90	90
	Mullite - 3% Ag	2.90	3.23	0.89	89	89
	Mullite - 5% Ag	2.93	3.28	0.89	89	89
	Mullite - 10% Ag	2.96	3.40	0.87	87	88
	Mullite - 20% Ag	3.38	3.68	0.91	91	96
	Mullite - 30% Ag	3.44	4.00	0.86	86	96

(A) Obtained by Archimedes method
(B) Calculated using the equation 5 with the nominal concentration of the silver.
(C) Equation 4, using the results of column B.
(D) $\rho_{relative}$ (column C) * 100
(E) $\rho_{relative}$ * 100, using the silver concentration (X_{silver}) obtained by EDS (Table III) in the equation 5.

If for the calculation of the densification we use the nominal concentrations of Ag we can see that this decreases to high silver concentration (20 and 30 wt%, 1500 and 1600 °C, Tab. I D) but this is not quite correct since the increase of the densification is usually associated with the decrease of the porosity (Fig. 3), a problem in the synthesis of cermets in the integration of metallic particles to the ceramic matrix [17], if in equation 2 we now use the concentration of Ag obtained by EDS (Tab. III) we can see that indeed the densification increases (Tab. I E) according to the porosity decrease (Fig. 3) which is consistent with the homogenization of the cermets microstructure observed by SEM (Fig. 4).

The variation of porosity as a function of silver concentration in the mullite/Ag cermets can be observed in Fig. 3, at 1500 °C the porosity decreases as the Ag concentration increases, starting with 15.77 % for mullite without silver to a minimum of 0.81 % at an Ag concentration of 20 %, although at 30 % Ag the porosity increases to 4.06 % (cermet 1500 °C mullite/30%Ag). However, at 1600 °C most of the cermets, in their different Ag contents, the porosity drops to values lose to 1 %, which suggests that the determining factor here is the

sintering temperature and with small amounts of silver we can obtain very low values of porosity, the highest value of porosity at 1600 °C is for the cermet with an Ag content of 10 % (cermet 1600 °C mullite/10%Ag). A similar behavior of the porosity was previously reported by Yu-Ming to the system corundum/mullite but as a function of temperature of sintered [31].

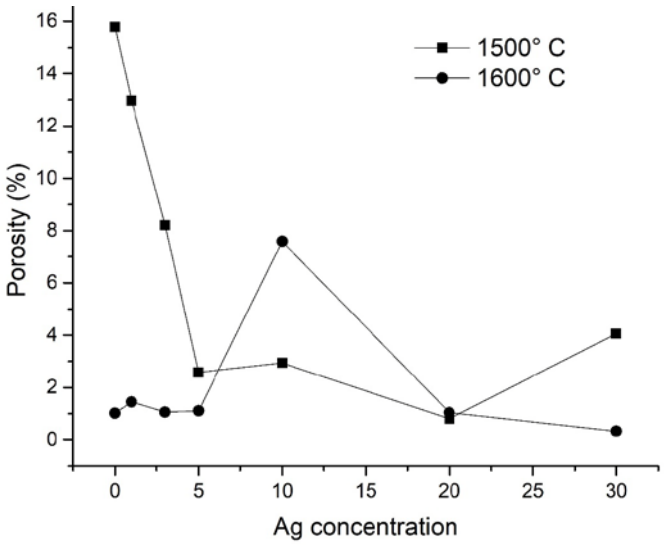

Fig. 3. Porosity as a function of the Ag concentration.

3.1 Microstructural characterization

An analysis by SEM/EDS was performed to observe the microstructural characteristics of the manufactured cermets as well as the homogenization of the grains of mullite by the sintering effect at the two different temperatures. It can be observed that at low concentrations of Ag (≤ 5 %) no significant changes in the microstructure and grain size were observed. It is possible to see two phases, gray and dark, in the micrographs of Fig. 4. the dark phase that delimits the phase gray is better defined at 1600 °C (Fig. 4 e, f, g and h) that at 1500 °C (Fig. 4 a, b, c, and d), the dark phase is not porosity because this decrease with the increase of Ag (Fig. 3) although we can think that is highly homogeneous phase because don´t have contrast, this effect is clear a high concentrations of silver (Fig. 4d and 4h) remembering that a back-scattered electron detector (BSE) was used to obtain these micrographs.

For 1600 °C mullite/10%Ag a change in its microstructure can be seen (Fig. 4g), this is associated with the increasing in its porosity (Fig. 3); meanwhile the cermet 1500 °C mullite-10% Ag only show a good separation of phases (gray and dark, Fig. 4c). At 1500 °C the transformation of microstructure is obtained with 20%Ag and with 30%Ag have a new microstructure with big grains (dark phase, Fig. 4d) but at 1600 °C this new microstructure appears since 20%Ag and 30%Ag (Fig. 4h) with a dark phase bigger, now the gray phase remains around the dark phase defining the new grain size, this indicate that the effect of the Ag addition is greater at 1600 °C.

The compositional analysis by EDS of the cermet 1600 °C mullite/30%Ag (general) and specifically of the phases dark (1) and gray (2) present in the Fig. 4h are shown in Tab. II. It can be observed that the gray phase has more oxygen, so we can assume that it is dissolved quartz around phase dark which is rich in Al and Si, so we can say that it is highly homogenized mullite, this homogenization was searched due to the addition of Ag and the sintering temperature. Silver dispersion is not observed in the micrographs of Fig. 4 due to its nanometric size and good dispersion as well integration in the grain boundaries of the mullite

matrix, however its presence was detected using EDS, the experimental concentration of Ag is shown in the Tab. III for all the sintered cermets.

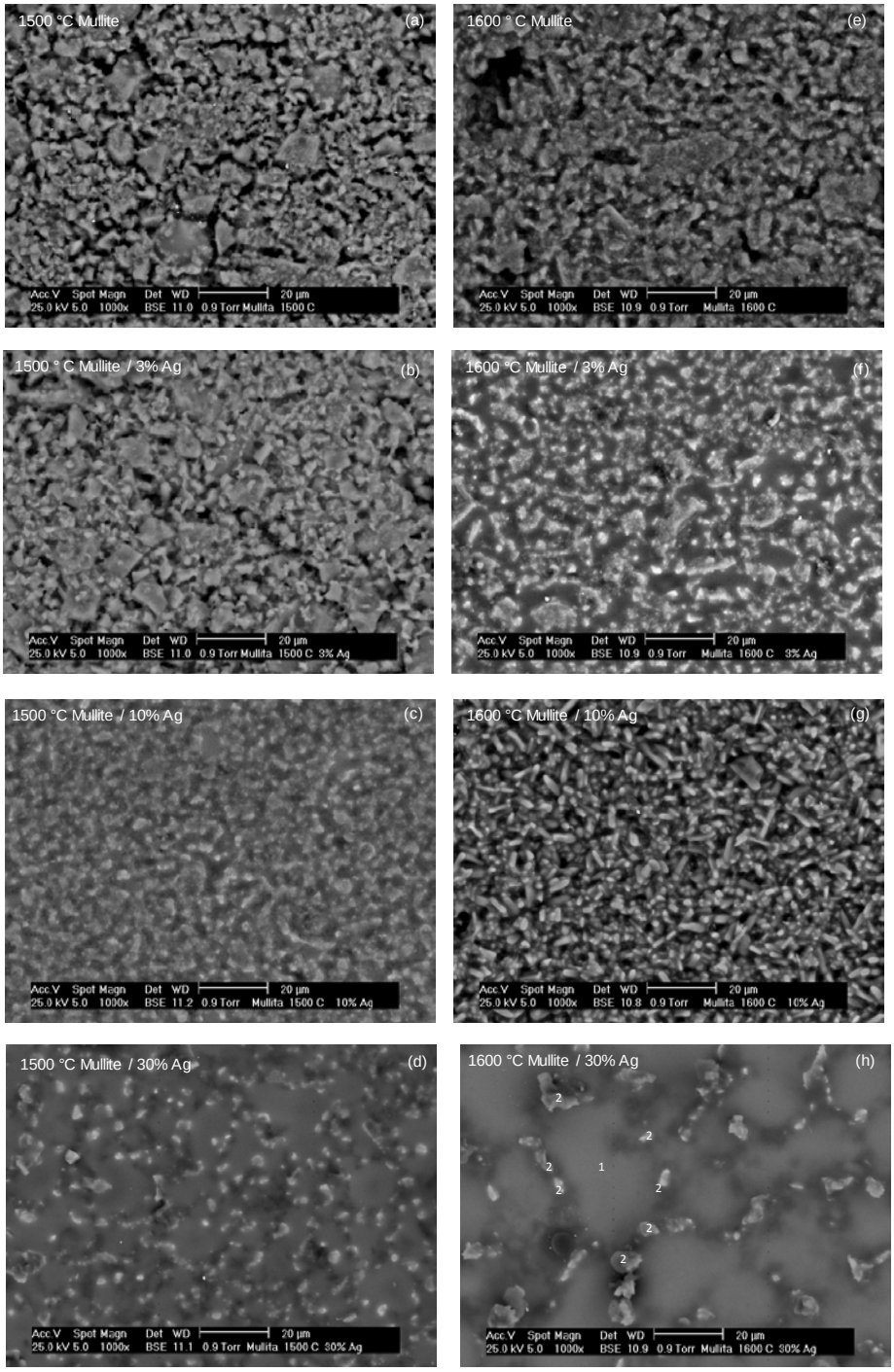

Fig. 4. SEM images of mullite/Ag at different concentrations and temperatures: (a) 1500 °C/0%Ag, (b) 1500 °C/3%Ag, (c) 1500 °C/10%Ag, (d) 1500 °C/30%Ag, (e) 1600 °C/0%Ag, (f) 1600 °C/3%Ag, (g) 1500 °C/10%Ag, and (h) 1600 °C/30%Ag.

Tab. II Phase´s Composition of Fig. 2h.

Element	% wt		
	General	1	2
O	40.90	39.96	49.55
Al	9.01	4.45	14.82
Si	33.36	34.27	26.33
Ag	15.44	20.07	8.38
Ti	1.29	1.25	0.93
Total	100	100	100

Tab. III EDS-SEM analysis for all sintered mullite/Ag cermets.

Sintered Temperature (°C)	Pads	Experimental concentration of Ag (% wt)
1500	Mullite	
	Mullite / 1% Ag	1.63
	Mullite / 3% Ag	3.09
	Mullite / 5% Ag	5.41
	Mullite / 10% Ag	10.24
	Mullite / 20% Ag	19.97
	Mullite / 30% Ag	21.31
1600	Mullite	
	Mullite / 1% Ag	1.24
	Mullite / 3% Ag	3.42
	Mullite / 5% Ag	5.13
	Mullite / 10% Ag	8.66
	Mullite / 20% Ag	14.57
	Mullite / 30% Ag	16.07

An alternative to know the distribution of Ag nanoparticles in the cermets is the technique of confocal scanning microscopy because in some opaque materials is possible obtain images and taking advantage of the reflection phenomenon of the laser in the metallic particles (Ag) to see the distribution of them in the ceramic matrix (mullite). In Fig. 5 we can observe the distribution of Ag nanoparticles in two cermets sintered at 1500 and 1600 °C with 10 %Ag concentration.

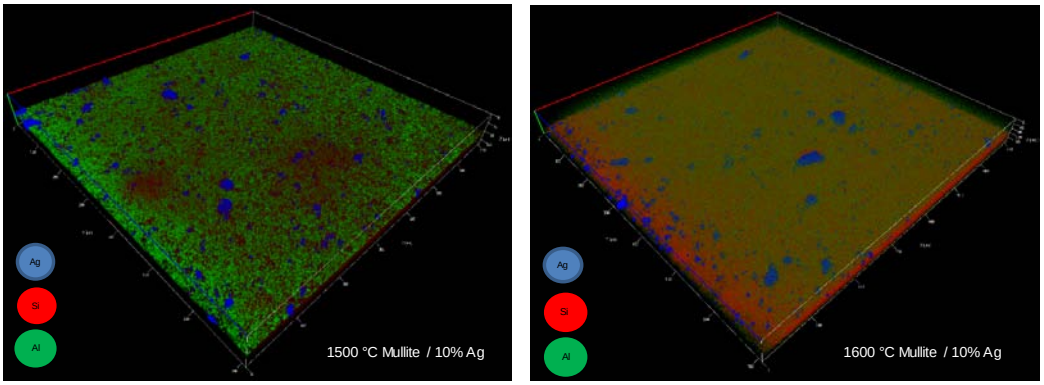

Fig. 5. Confocal laser scanning microscopy images of the mullite/10%Ag sintered at 1500 and 1600 °C.

3.2 X-Ray Diffraction Analysis

Due to the high sintering temperatures of the cermets (1500 and 1600 °C) compared to the melting temperature of the mullite (1830 °C), X-ray diffraction was performed to verify the stability of the cermets and/or possible phase transitions as well as the presence of silver. In all the cermets it can be verified that the mullite phase is maintained independently of the sintering temperature and Ag concentration, peaks of other phases (another aluminosilicate) not appear (Fig. 6 and Fig. 7), consequently the two phases observed in SEM (gray and dark) correspond to the mullite with the difference that the dark phase is homogenized mullite and as it increases the silver content increases.

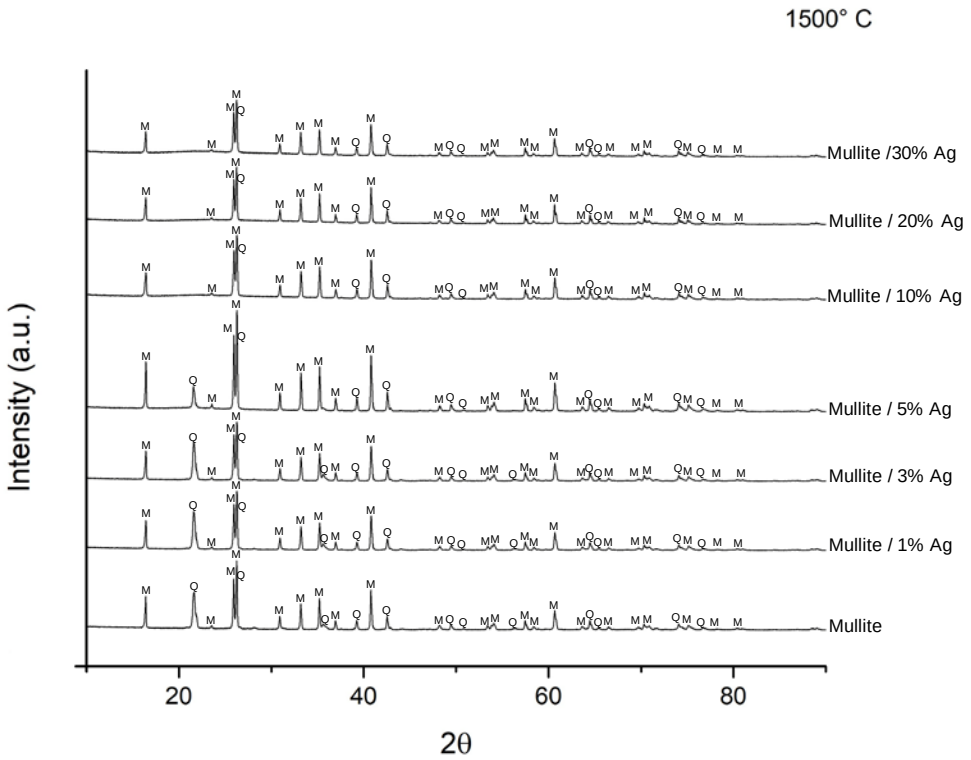

Fig. 6. XRD pattern of the mullite/Ag cermets sintered at 1500 °C.

In the case of the diffraction peak of the Ag this is not appreciated due to the nanometric size of its crystals since overlaps with those of mullite, regardless of the concentration of Ag in the cermets. What is important to note is the presence of quartz in the mullite, in cermets sintered at 1500 °C this can be seen in cermets with concentrations of up to 5% Ag, for cermets with 10, 20 and 30 % of Ag no longer detects the presence of quartz, in the case of cermets sintered at 1600 °C only the quartz peak is seen in the cermet that has no silver, because the quartz melting temperature is 1713 °C is not may think that it has melted but only scattered and diffused in the mullite matrix by the combined action of temperature and silver in the cermets, at 1600 °C only the temperature is necessary to cause this phenomenon, while for 1500 °C It is necessary low concentrations of Ag with temperature to cause this phenomenon.

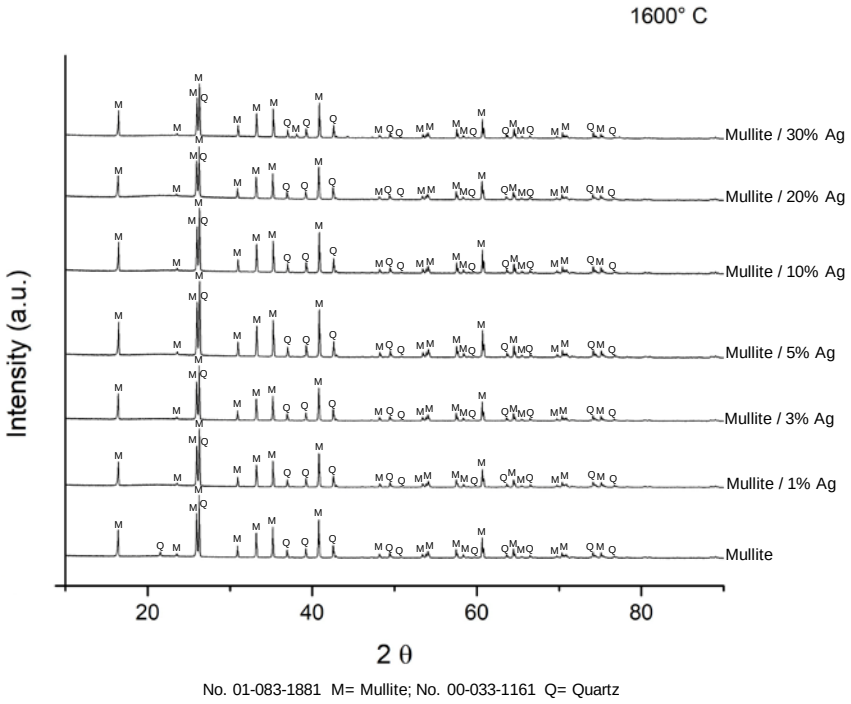

Fig. 7. XRD pattern of the mullite/Ag cermets sintered at 1600 °C.

3.3 Mechanical Properties

Tab. IV Hardness and fracture toughness.

Sintered Temperature (°C)	Pads	Young's module (GPa)	Speed of sound (m/s)	Vickers Hardness (HV)	Fracture Toughness Kc ($MPa \cdot m^{1/2}$)
1500	Mullite	133.87	6877.71	731 ± 48	1.90
	Mullite / 1% Ag	118.77	6455.50	1022 ± 29	1.38
	Mullite/ 3% Ag	106.84	6090.57	1010 ± 33	2.02
	Mullite / 5% Ag	122.32	6483.14	949 ± 35	1.61
	Mullite / 10% Ag	117.59	6313.57	940 ± 20	1.71
	Mullite / 20% Ag	85.16	5191.33	901 ± 23	1.74
	Mullite / 30% Ag	108.11	5785.43	887 ± 44	2.16
1600	Mullite	108.75	6166.33	1171 ± 27	1.38
	Mullite / 1% Ag	154.77	7330.67	1244 ± 24	1.63
	Mullite / 3% Ag	117.04	6352.83	1044 ± 32	1.56
	Mullite / 5% Ag	146.53	7071.71	964 ± 40	2.42
	Mullite / 10% Ag	147.72	7064.43	960 ± 40	2.12
	Mullite / 20% Ag	158.44	6390.33	934± 54	2.41
	Mullite / 30% Ag	105.68	5542.57	888 ± 41	1.77

Tab. IV shows the results of Vickers hardness (HV) and fracture toughness (K_c). For mullite/Ag cermets, at both sintering temperatures the highest hardness values are: 1022 for

1500 Mullite/1% Ag cermet and 1244 for 1600 Mullite/1% Ag with P_H = 0.2 Kgf (1.96N); in this work, the hardness tends to decrease as the content of Ag increases, behavior similar to that observed with the densification. Fracture toughness K_c was determined by indentation applying a load of P_{FT} = 0.5 Kgf (4.90 N), at 1500 °C there is a maximum of 2.02 MPa.$m^{1/2}$ for the 1500 Mullite/3% Ag cermet, with the 1500 Mullite/5%Ag cermet it decreases its value at 1.61 MPa.$m^{1/2}$ to grow again until a second maximum of 2.16 MPa.$m^{1/2}$ with 1500 Mullite/30%Ag cermet. For the cermets sintered at 1600 °C the fracture toughness starts with a value of 1.38 MPa.$m^{1/2}$ for the cermet 1600 mullite (without Ag) and reaches a maximum of 2.42 MPa.$m^{1/2}$ with 1600 Mullite/5%Ag cermet, at higher concentrations the fracture toughness decreases. At both temperatures the fracture toughness increases as the Ag content increases but in two stages, at low and high concentration, at 1500 °C the first stage is in the range of 0 to 3 % and the second one from 5 to 30 % of Ag, while at 1600 °C it is from 0 to 5 % from 10 to 30 % respectively. The two stages in which the fracture toughness presents can easily be associated with the microstructure changes shown in Fig. 4. Moya et al. [17, 24] found that the fracture resistance in the mullite-Mo system depends on the volume fraction of the metal and the grain size of the matrix, meanwhile Kawasaki et al. [32] tell us that the fracture toughness K_c, increases as the metallic phase content increases in the ceramic matrix. Traits that are considered relevant for determining the increase in hardness and fracture toughness include the volume fraction of the second phase, the morphology and size of the particle and the aspect ratio, and the spatial distribution of the particles.

4. Conclusion

The incorporation of Ag in mullite at both sintering temperatures, 1500 and 1600 °C increases the fracture toughness but in two stages, at low and high concentration, these two stages in which we can divide the behavior of the fracture toughness can be associated with microstructure changes observed by SEM like changes in the shape, increasing size and homogenization of the mullite grain and by confocal microscopy in the distribution of the Ag in the mullite, all these effects are greater at 1600°C.

Acknowledgments

The authors would like to thank to Universidad Michoacana de San Nicolas de Hidalgo (UMSNH) for the support and facilities of this research.

5. References

1. H. Schneider, J. Schreuer and B. Hildmann, J. Eur. Ceram. Soc., 28 (2008) 329-344.
2. I. A. Aksay, D. M. Dabbs, and M. Sarikaya, J. Am. Ceram. Soc., 74 (10) (1991) 2343-2358.
3. J. Roy, S. Das and S. Maitra, Int. J. Appl. Ceram. Technol., 12 (S2) (2015) 71-77.
4. T. Ebadzadeh, Mat. Sci. Eng.: A, 355 (1-2) (2003) 56-61.
5. F. A. Costa Oliveira, V. Livramento and F. Delmas, J. Mat. Process Tech., 195 (2008) 255-259.
6. N. M. Rendtorff, L. B. Garrido and E. F. Aglietti, Ceramics International, 35 (7) (2009) 2907-2913.
7. Tai-Il. Mah and Mazdiyasni, K. S., J. Am. Ceram. Soc., 66 (10) (1983) 699-703.
8. S. Kanzaki, H. Tabata, T. Kumazawa, and S. Ohta, J. Am. Ceram. Soc., 68 (1) (1985) C-6-C-7.

9. M. G. M. U. Ismail, Z. Nakai and S. Somiya, J. Am. Ceram. Soc., 70 (1) (1987) C-7-C-8.
10. M. A. Camerucci, G. Urretavizcaya, M. S. Castro and A. L. Cavalieri, J. Eur. Ceram. Soc., 21 (2001) 2917-2923.
11. M. Mohammed, C. M. Hoo, M. L. Mecartney and H. Schneider, J. Am. Ceram. Soc., 97 (6) (2014) 1923-1930.
12. M. M S. Sanad, M. M. Rashad, E. A. Abdel-Aal, M. F. El-Shahat, Ceramic International, 39 (2) (2013) 1547-1554.
13. R. Torrecillas, G. Fantozzi, S. De Aza and J. S. Moya, Acta Mater., 45 (3) (1997) 897-906.
14. H. Schneider and S. Komarneni, Mullite, Wiley-VCH, Weinheim. 2005.
15. H. Ashrafi, R. Emadi, R. Zamani and R. Foroushani, Adv. Powder Tech., 26 (2015) 1452-1457.
16. K. A. Khor, L. G. Yu, Y. Li, Z. L. Dong and Z. A. Munir, Mat. Sci. Eng. A339 (1-2) (2003) 286-296.
17. J. S. Moya, S. Lopez-Esteban and C. Pecharromán, Progress in Materials Science, 52 (7) (2007) 1017-1090.
18. S. William and J. HashemI, Fundamentos de la Ciencia e Ingeniería de Materiales, Mc Graw Hill, 2004.
19. N. Rendtorff, Materiales cerámicos del sistema Mullita Zirconia Zircón; propiedades mecánicas, de fractura y comportamiento frente al choque térmico, Tesis doctoral 2009, Universidad Nacional de Plata.
20. M. Szafran, K. Konopka, E. Bobryk and K. J. Kurzydłowski, J. Eur. Ceram. Soc., 27 (2–3) (2007) 651-654.
21. J. F. Bartolomé, M. Díaz and J. S. Moya, J. Am. Ceram. Soc., 85 (11) (2004) 2778-2784.
22. L. B. Kong, H. Huang, T. S. Zhang, Y. B. Gan, J. Ma, F. Boey and R. F. Zhang. Mater. and Eng. A359 (2003) 75-81.
23. D. D. Jayaseelan, D. A. Rani, T. Nishikawa, H. Awaji and T. Ohji, J. Eur. Ceram. Soc., 22 (7) (2002) 1113-1117.
24. J. S. Moya, M. Díaz, C. F. Gutiérrez-González, L.A. Diaz, R. Torrecillas and J. F. Bartolomé, J. Eur. Ceram. Soc., 28 (2008) 479-491.
25. H. Zhang, N. Maljkovic and B. S. Mitchell, Mater. Sci. Eng. A326 (2002) 317-323.
26. N. Mansourirad, M. Ardestani and M. R. Afshar, Science of Sintering, 50 (2018) 323-335.
27. C. Marambio-Jones, E. M. V. Hoek, J. Nanopart. Res., 12 (2010) 1531-1551.
28. J. G. Ayala-Landeros, V. Saucedo-Rivalcoba, S. Bribiesca-Vasquez, V.M. Castaño, A. L. Martínez-Hernández, C. Velasco-Santos, Science of Sintering, 48 (2016) 29-39.
29. JIS R 1607, "Testing Methods for Fracture Toughness of High Performance Ceramics," Japanese Standards Association, Tokyo, 1990.
30. T. Miyoshi, Trans. Jap. Soc. Mech. Eng, Series A, 51A (1985) 2489-2497.
31. T. Yu-Ming, Z. Peng-fei, K. Xiang-chen, L. Ai-ping, W. Kai-yue, C. Yue-sheng, L. Zhan-gang, L. V. De-fu, Science of Sintering, 47 (2015) 273-278.
32. A. Kawasaki and R. Watanabe, Eng. Fract. Mechan., 69 (2002) 1713-1728.

Садржај: *Циљ овог рада био је испитивање утицаја додатка наночестица сребра у микроструктуру мулита на две различите температуре синтеровања (1500 и 1600 °C), да би се смањила порозност, повећала густина као и чврстоћа. Микроструктурне карактеристике су испитиване скенирајућом електронском микроскопијом и рендгенском дифракцијом. Мулит/Ag кермети са хомогеном структуром су показали жилавост лома од 2,42 MPa•m$^{1/2}$.*

***Кључне речи**: мулит, конфокална скенирајућа микроскопија, скенирајућа електронска микроскопија, хомогена микроструктура, синтеровање.*